

# Three-Dimensional Echocardiography and 2D-3D Speckle-Tracking Imaging in Chronic Pulmonary Hypertension: Diagnostic Accuracy in Detecting Hemodynamic Signs of Right Ventricular (RV) Failure

Antonio Vitarelli, MD; Enrico Mangieri, MD; Claudio Terzano, MD; Carlo Gaudio, MD; Felice Salsano, MD; Edoardo Rosato, MD; Lidia Capotosto, MD; Simona D'Orazio, MD; Alessia Azzano, MD; Giovanni Truscilli, MD; Nino Cocco, MD; Rasul Ashurov, MD

**Background**—Our aim was to compare three-dimensional (3D) and 2D and 3D speckle-tracking (2D-STE, 3D-STE) echocardiographic parameters with conventional right ventricular (RV) indexes in patients with chronic pulmonary hypertension (PH), and investigate whether these techniques could result in better correlation with hemodynamic variables indicative of heart failure.

**Methods and Results**—Seventy-three adult patients (mean age, 53±13 years; 44% male) with chronic PH of different etiologies were studied by echocardiography and cardiac catheterization (25 precapillary PH from pulmonary arterial hypertension, 23 obstructive pulmonary heart disease, and 23 postcapillary PH from mitral regurgitation). Thirty healthy subjects (mean age, 54±15 years; 43% male) served as controls. Standard 2D measurements (RV-fractional area change–tricuspid annular plane systolic excursion) and mitral and tricuspid tissue Doppler annular velocities were obtained. RV 3D volumes and global and regional ejection fraction (3D-RVEF) were determined. RV strains were calculated by 2D-STE and 3D-STE. RV 3D global-free-wall longitudinal strain (3DGFW-RVLS), 2D global-free-wall longitudinal strain (GFW-RVLS), apical-free-wall longitudinal strain, basal-free-wall longitudinal strain, and 3D-RVEF were lower in patients with precapillary PH ( $P<0.0001$ ) and postcapillary PH ( $P<0.01$ ) compared to controls. 3DGFW-RVLS (hazard ratio 4.6, 95% CI 2.79 to 8.38,  $P=0.004$ ) and 3D-RVEF (hazard ratio 5.3, 95% CI 2.85 to 9.89,  $P=0.002$ ) were independent predictors of mortality. Receiver operating characteristic curves showed that the thresholds offering an adequate compromise between sensitivity and specificity for detecting hemodynamic signs of RV failure were 39% for 3D-RVEF (AUC 0.89), –17% for 3DGFW-RVLS (AUC 0.88), –18% for GFW-RVLS (AUC 0.88), –16% for apical-free-wall longitudinal strain (AUC 0.85), 16 mm for tricuspid annular plane systolic excursion (AUC 0.67), and 38% for RV-FAC (AUC 0.62).

**Conclusions**—In chronic PH, 3D, 2D-STE and 3D-STE parameters indicate global and regional RV dysfunction that is associated with RV failure hemodynamics better than conventional echo indices. (*J Am Heart Assoc.* 2015;4:e001584 doi: 10.1161/JAHA.114.001584)

**Key Words:** chronic pulmonary hypertension • echocardiography • right ventricular function • speckle-tracking echocardiography • three-dimensional echocardiography

Quantitative echocardiographic assessment of right ventricular (RV) function is becoming of increasing interest in cardiac diseases that affect the right ventricle, such as congenital heart disease and acute or chronic pulmonary hypertension (PH),<sup>1,2</sup> but is still challenging due to RV complex anatomy and structure. Evaluation of RV function is particularly important in chronic PH since the primary cause

of death is RV failure that is highly associated with RV parameters such as cardiac index and right atrial (RA) pressure. Two-dimensional (2D) echocardiographic methods of analyzing RV performance employ geometric models that do not represent the irregular RV shape accurately. Real-time 3-dimensional echocardiography (3DE) allows us to measure RV end-diastolic volume and ejection fraction (3D-RVEF) irrespective of its shape and more reliably compare it to 2-DE<sup>3–5</sup> and evaluate the morphologic and functional remodeling of the right ventricle in PH. Tissue Doppler imaging and 2-dimensional speckle-tracking echocardiography (2D-STE) are new means of evaluation of myocardial wall movements and deformation, and it has been suggested that the use of indexes derived from STE can be proposed as an adjunctive tool in the overall assessment of RV function.<sup>6–9</sup> 2D-STE capability is limited by the changes in heart morphology during the cardiac cycle and the difficulty in tracking speckles

From the Sapienza University, Departments of Cardiology (A.V., E.M., C.G., L.C., S.D'O., A.A., G.T., N.C., R.A.), Pneumology (C.T.), and Medicine (F.S., E.R.), Italy.

**Correspondence to:** Antonio Vitarelli, MD, Via Lima 35, 00198 Rome, Italy. E-mails: vitar@tiscali.it, cardiodiagnostica@gmail.com

Received November 1, 2014; accepted February 20, 2015.

© 2015 The Authors. Published on behalf of the American Heart Association, Inc., by Wiley Blackwell. This is an open access article under the terms of the Creative Commons Attribution-NonCommercial License, which permits use, distribution and reproduction in any medium, provided the original work is properly cited and is not used for commercial purposes.

in different frames because of out-of-plane motion. The newly developed 3-dimensional speckle-tracking echocardiography (3D-STE) provides quick and comprehensive quantitative assessment of ventricular myocardial dynamics and was applied to the study of the right ventricle in PH.<sup>10,11</sup> However, the hemodynamic value of these new echocardiographic parameters in the clinical setting of PH and RV failure was not clearly established. Accordingly, we sought to analyze the use of 3DE, 2D-STE, and 3D-STE in the assessment of global and regional RV function in patients with chronic PH to evaluate whether these parameters could detect hemodynamic signs of RV failure better than conventional echo indices.

## Methods

### Population

We enrolled 73 patients with chronic PH, as defined by the Task Force of the European Society of Cardiology and American Heart Association.<sup>1,2</sup> The etiology of PH is listed in Table 1. Precapillary or postcapillary PH was diagnosed according to current guidelines on the basis of the invasive hemodynamic evaluation.<sup>1</sup> Patients with precapillary PH were patients with mean pulmonary arterial pressure  $\geq 25$  mm Hg and pulmonary capillary wedge pressure  $\leq 15$  mm Hg; patients with postcapillary PH were patients with mean pulmonary arterial pressure  $\geq 25$  mm Hg and pulmonary capillary wedge pressure  $> 15$  mm Hg. Forty-eight patients had precapillary PH; 25 of them had pulmonary arterial hypertension (PAH), and 23 had chronic obstructive pulmonary disease (COPD). Of PAH patients, 13 had congenital heart disease (ostium secundum atrial septal defect 4 patients, VSD 3 patients, PDA 2 patients, residual shunt from postoperative ostium primum atrial septal defect 2 patients), and 12 had systemic sclerosis. Congenital PH patients had no prior surgery that required operative manipulation of the RV. Twenty-five patients had postcapillary PH from mitral regurgitation (MR). Exclusion criteria included cardiomyopathy, atrial fibrillation, comorbidities, pregnancy, and insufficient ultrasound image quality (defined as more than 3 myocardial segments that were not optimally visualized using conventional 2DE). Patients were followed up with mortality data and assessed at 24 months. The mean follow-up period was 3.6 years (median 2.8 years). Information about symptoms and functional class (according to the New York Heart Association) was collected. Thirty healthy age- and sex-matched adults who had no histories of cardiopulmonary disease, no known coronary risk factors, and normal electrocardiographic and echocardiographic results, were selected as a control group. The study was approved by the Institutional Medical Research Committees. Written informed consent was obtained.

### Standard Echocardiography

All patients underwent transthoracic echocardiography with a commercially available cardiovascular ultrasound system (Vivid E9; GE, Horten, Norway). Established criteria were used for measurements of left and right chambers.<sup>12</sup> 2D and M-mode left ventricular (LV) dimensions were obtained. Doppler mitral peak early (E) and late (A) diastolic velocities, and tissue Doppler imaging mitral valve annulus velocities (MV  $S_a$ ,  $E_a$ ,  $A_a$ ) were measured on the transthoracic 4-chamber views. MV E/ $E_a$  ratio is a parameter reflecting LV filling pressure<sup>12</sup> and was determined by measuring velocities of the lateral mitral valve annulus. RV to LV end-diastolic diameter ratio was calculated in the apical 4-chamber view. RV end-diastolic area and end-systolic area were assessed by manual planimetry, and RV fractional area change (RVFAC) was derived using the formula  $RVFAC = [(RVEDarea - RVESarea) / RVEDarea] \times 100$  (where ED=end diastolic and ES=end systolic). Tricuspid annular plane systolic excursion (TAPSE) was measured using apical views adjusted to optimize RV structures and to achieve proper orientation for M-mode measures. Myocardial performance index was derived from the analysis of RV function Doppler parameters. Pulmonary acceleration time (PAT) was measured as the interval between the onset of ejection and peak pulmonary flow velocity from the parasternal short-axis view. Right ventricular systolic pressure (RVSP) was determined by continuous-wave Doppler echocardiography and was considered elevated when reaching values  $> 30$  mm Hg. RA pressure was estimated according to caval dimensions. Estimation of pulmonary vascular resistance (PVR) was determined on the basis of the ratio of peak tricuspid regurgitation velocity to RV outflow tract time-velocity integral that was shown to be a good correlate of PVR despite reflecting pulmonary systolic pressure and not the transpulmonary pressure gradient.<sup>13</sup> Pulmonary artery capacitance was calculated as Doppler-derived stroke volume/pulmonary artery pulse pressure.<sup>14</sup> Tricuspid annulus systolic velocity (TV  $S_a$ ) and diastolic velocity (TV  $E_a$ ) were measured at the lateral corner of the tricuspid annulus on the transthoracic 4-chamber view. TV E/ $E_a$  reflects increased RA pressure<sup>12,15</sup> and was taken as the parameter of RV diastolic function

### Three-Dimensional Echocardiography

3DE was done using a dedicated wide-angle, broadband matrix-array transducer to allow for full cover of the entire RV by the pyramidal volume, with special attention to the outflow tract and upper anterior wall. Before acquisitions, images were optimized for the endocardial border visualization, modifying overall gain and adjusting time gain and compression. Then they were digitally stored for offline analysis by TomTec software (TomTec Imaging Systems, Unterschleissheim, Germany).

**Table 1.** Baseline Characteristics of Pulmonary Hypertension Patients and Normal Controls

	PAH (n=25)		COPD (n=23)	MR (n=25)	Controls (n=30)	P Value
	SS (n=12)	CHD (n=13)				
Age, y	53±11	52±13	55±14	51±11	54±15	ns
Sex, M/F	5/7	6/7	10/13	11/14	13/17	ns
BSA, m <sup>2</sup>	1.84±0.13	1.82±0.15	1.89±0.17	1.84±0.11	1.87±0.16	ns
BMI, kg/m <sup>2</sup>	23±4	22±5	23±4	22±5	23±3	ns
HR, beats/min	74±10	72±11	74±9	73±11	65±8	ns
NYHA-FC III/IV	4 (33%)	3 (25%)	6 (26%)	8 (32%)	—	ns
SBP, mm Hg	116±13	119±14	121±11	120±16	114±15	ns
DBP, mm Hg	67±9	67±10	69±10	65±7	63±8	ns
Mean RAP, mm Hg	15.3±4.9	14.2±5.1	13.2±3.8	11.4±4.4	—	<0.05*
Systolic PAP, mm Hg	66.1±16.8	64.5±14.3	47.2±11.8	42.7±12.4	—	<0.05 <sup>†</sup> , <0.01 <sup>‡</sup>
Diastolic PAP, mm Hg	25.9±11.9	25.3±10.1	24.2±7.8	22.7±6.4	—	ns
Mean PAP, mm Hg	44.9±10.3	42.1±9.4	37.8±5.3	32.9±4.9	—	<0.05* <sup>§</sup>
PCWP, mm Hg	8.7±3.6	8.9±3.9	7.4±3.1	22.6±3.8	—	<0.001*
TPG, mm Hg	36.1±11.6	33.4±13.2	31.2±9.3	10.2±4.8	—	<0.005* <sup>§</sup>
PAC, mL/mm Hg	0.8±0.2	1.1±0.3	1.7±0.8	2.8±0.7	—	<0.001* <sup>§</sup>
PVR, WU	5.9±2.3	5.2±2.4	3.9±0.8	1.7±0.4	—	<0.05 <sup>†§</sup> , <0.005 <sup>‡</sup>
CI, L/min per m <sup>2</sup>	2.3±0.5	2.4±0.4	2.6±0.5	3.4±0.5	—	<0.05*

BMI indicates body mass index; BSA, body surface area; CHD, congenital heart disease; CI, cardiac index; COPD, chronic obstructive pulmonary disease; DBP, diastolic blood pressure; HR, heart rate; MR, mitral regurgitation; ns, not statistically significant; NYHA-FC, New York Heart Association functional class; PAC, pulmonary artery capacitance; PAH, pulmonary arterial hypertension; PAP, pulmonary artery pressure; PCWP, pulmonary capillary wedge pressure; PVR, pulmonary vascular resistance; RAP, right atrial pressure; SBP, systolic blood pressure; SS, systemic sclerosis; TPG, transpulmonary pressure gradient; WU, Wood units.

\*SS, CHD, and COPD vs MR.

<sup>†</sup>SS and CHD vs COPD.

<sup>‡</sup>SS and CHD vs MR.

<sup>§</sup>SS vs CHD.

Three orthogonal planes and various landmarks were selected to define the end-diastolic and end-systolic frames. The program automatically supplies 4-chamber, sagittal, and coronal RV views on the basis of the initial view adjustment. RVEDV and RVESV were calculated from 3D echocardiographic data sets. RVEF was determined as follows:  $RVEF = [(RVEDV - RVESV) / RVEDV] \times 100$  (Figure 1). Total RVEF was automatically generated by the software. Inflow, outflow, and apex RVEFs were measured by subtracting the minimum (end-systolic) volume from the maximum (end-diastolic) volume of the respective compartment divided by the end-diastolic volume. Volume changes during the cardiac cycle were assessed.

### Speckle-Tracking Echocardiography

The general principles that underlie 2D speckle-tracking modalities have been previously described.<sup>15–21</sup> Patients were placed in the left lateral decubitus position and examined with an active matrix single-crystal phased-array transducer (GE-M5S). Grayscale recordings were optimized at a mean frame

rate of  $\geq 50$  frames/s. Apical 4-chamber views were used to assess the RV inflow compartment, and special care was taken to ensure a proper image of the entire RV by narrowing the width of the 2D sector, or by placing the transducer in 1 intercostal space lower and side. To assess regional and global longitudinal RV systolic function, we adopted a 6-segment RV model (basal RV free wall, mid RV free wall, apical RV wall, apical septum, mid septum, and basal septum). Peak systolic strain was recorded for the 3 RV myocardial free wall and septal segments, and the entire RV wall and RV free-wall segments were selected for measurements (Figure 2). RV outflow compartment was assessed by tracing along the right ventricular outflow tract wall in parasternal short axis views as previously described<sup>20</sup> and displaying the corresponding segmental and global strain curves. Time to peak negative strain with respect to the onset of the Q-wave of the superimposed ECG was measured for inflow and outflow segments. The echocardiographic results were analyzed by an echocardiologist (A.V.) blinded to the clinical data, using dedicated software (EchoPAC BT12, 4D Auto LVQ; GE Vingmed Ultrasound, Horten, Norway).

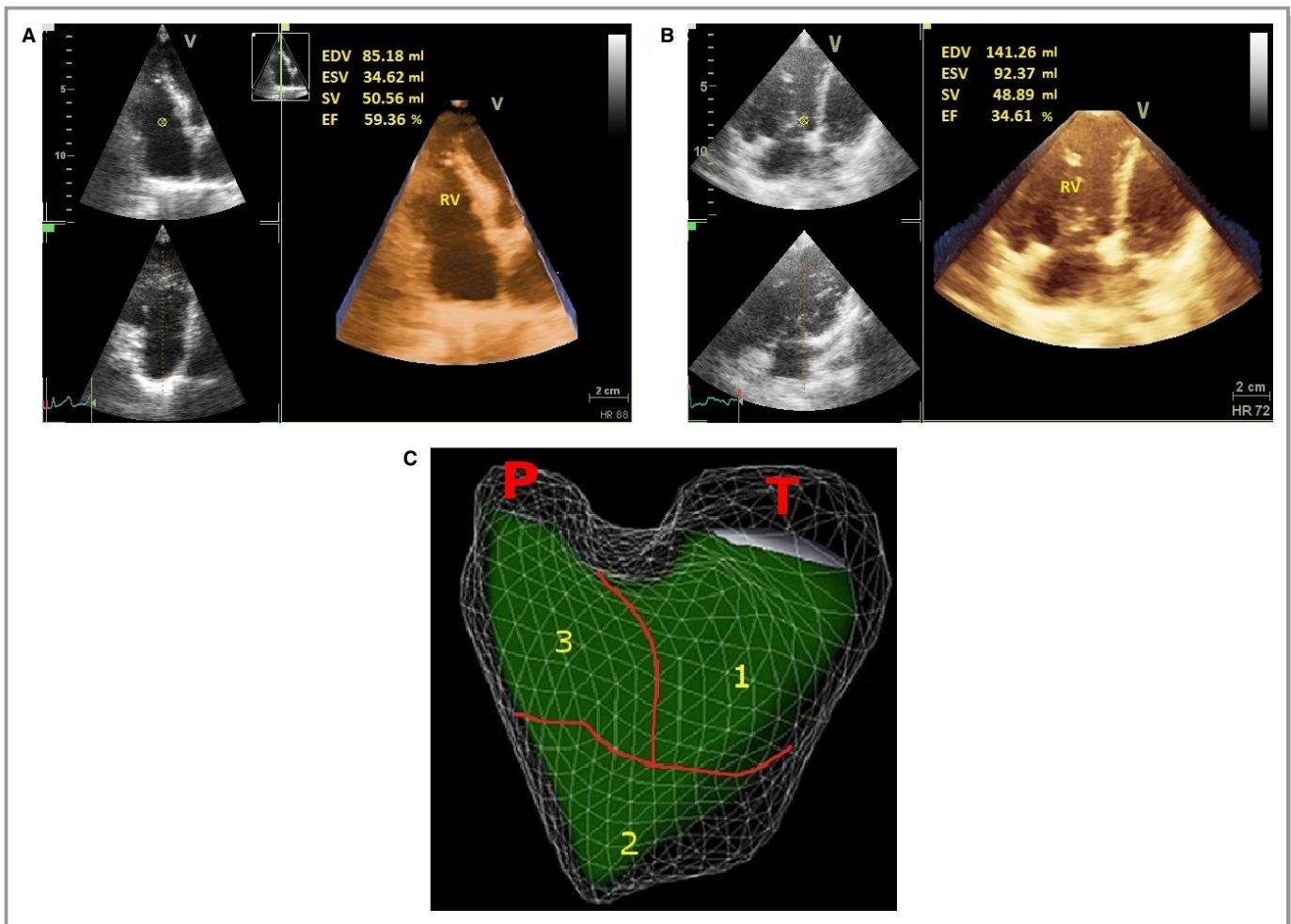


**Figure 1.** Representative 3D RV volumes and ejection fraction in normal controls and PH patients. A, Three-dimensional RV ejection fraction (3D-RVEF) in a normal subject. 3D-RVEF=59%. B, Decrease of 3D-RVEF in a patient with chronic PH. 3D-RVEF=35%. C, Regional three-dimensional RV ejection fraction. RV components are illustrated in a three-dimensional reconstruction of the echocardiographic images seen in a front view. 1, inlet; 2, apical trabecular; 3, outlet component. EDV indicates end-diastolic volume; EF, ejection fraction; ESV, end-systolic volume; P, pulmonary outflow; PH, pulmonary hypertension; RV, right ventricular; RVEF, RV ejection fraction; SV, stroke volume; T, tricuspid inflow.

3D speckle-tracking analysis was performed after imaging the RV chamber in apical views by using a 4V phased array transducer with high volume rate ( $\geq 30$  image frames/s) and 6-beat acquisition. 3D global longitudinal strain of whole RV (17 segments) was calculated using the Echo PAC BT12 (Figure 2). 3D global longitudinal strain of RV free-wall only (3D Global-FW RVLS) was calculated using Excel data.<sup>10</sup> 3D global area strain (AS) was determined as the percentage decrease in the size of endocardial surface area defined by the vectors of longitudinal and circumferential deformations.<sup>11</sup> 3D global area strain of RV free-wall only (3D Global-FW AS) was then calculated.

### Cardiac Catheterization

PH was confirmed by cardiac catheterization and right-heart hemodynamic measurements. These studies were performed

under fluoroscopic guidance via a femoral vein approach within 3 days of echocardiography with a mean interval of  $1.4 \pm 0.4$  days. Measurements were obtained at end expiration after zero-pressure calibration and included right atrial, pulmonary arterial peak systolic and end-diastolic, and pulmonary capillary wedge pressures. Mean pulmonary artery pressure, PVR, transpulmonary pressure gradient (mean pulmonary artery pressure minus mean wedge pressure), and pulmonary artery capacitance (ratio of stroke volume over pulmonary pulse pressure) were calculated. Cardiac output was determined by thermodilution<sup>22</sup> and indexed to body surface area to obtain cardiac index.

### Statistics

Categorical variables are presented as numbers and percentages and continuous data are expressed as mean  $\pm$  SD.

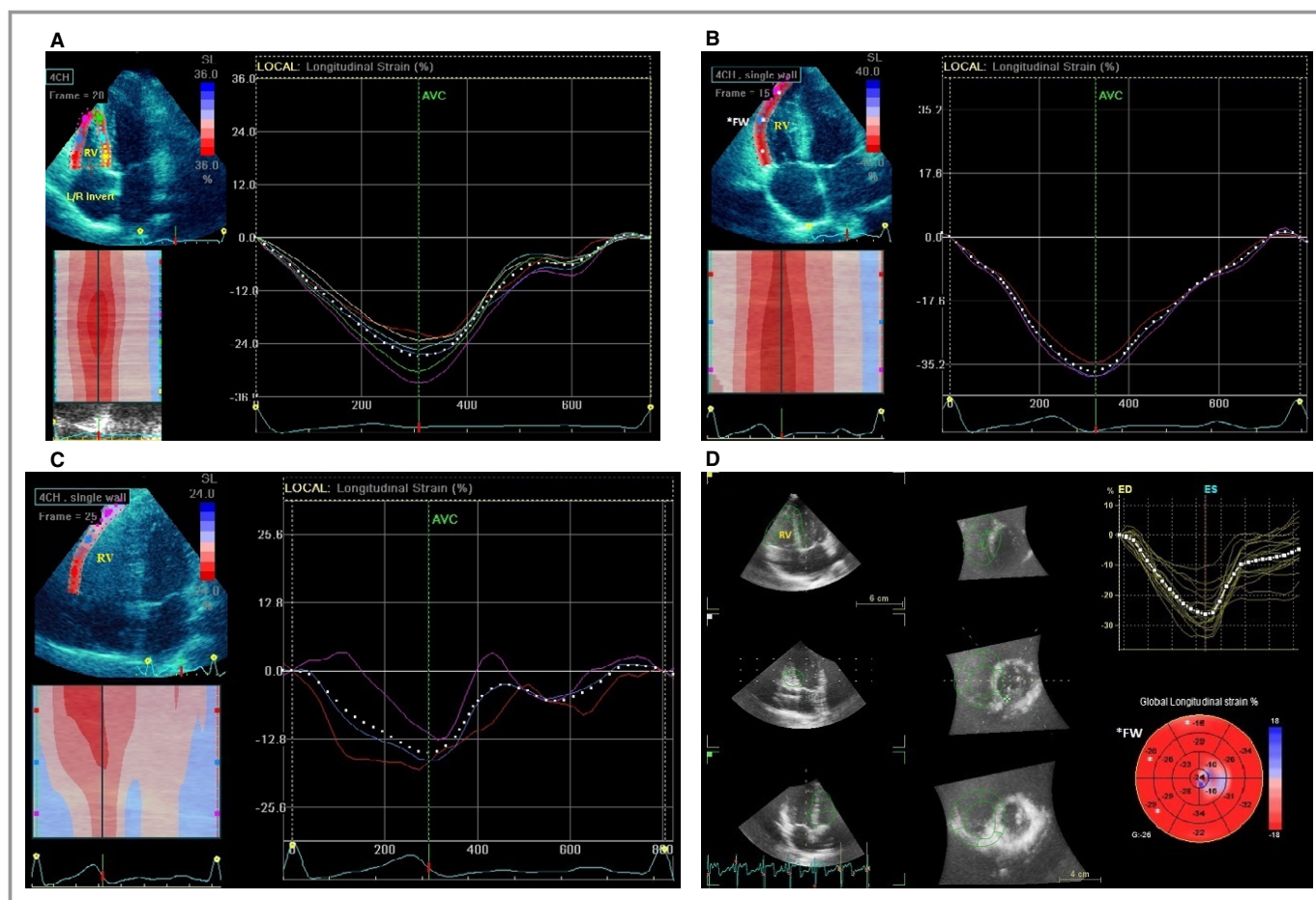


**Figure 2.** Representative 2D and 3D RV strain images in normal controls and PH patients. A, Speckle-tracking apical view showing global and regional RV longitudinal strain in a normal subject. Global RV longitudinal strain (G-RVLS) =  $-28\%$ . B, Speckle-tracking apical view showing global and regional free-wall RV longitudinal strain in a normal subject. Free wall (FW) is labeled by asterisks. Global free-wall RV longitudinal strain (GFW-RVLS) =  $-36\%$ . C, Decrease of GFW-RVLS in a patient with chronic PH. GFW-RVLS =  $-13\%$ . D, 3D RV speckle-tracking multiplane view in a normal subject. 3D global longitudinal strain (3D G-RVLS) was  $-26\%$ . 3D global longitudinal strain of RV free-wall (3D GFW-RVLS) was then calculated excluding septal segments. FW is labeled by asterisks. AVC indicates aortic valve closure; ED, end-diastolic; ES, end-systolic; PH, pulmonary hypertension; RV, right ventricular.

Patients were divided into 5 groups (systemic sclerosis, congenital heart disease, COPD, mitral regurgitation, and controls). Echocardiographic parameters of RV function (standard, STE, 3D) as well as cardiac catheterization parameters were compared between groups using Student unpaired *t* tests. Differences among 3 or more groups were assessed using 1-way ANOVA. Differences were considered statistically significant when the *P* value was  $<0.05$ . Cox proportional hazards regression models were used to identify clinical, echocardiographic, and invasive hemodynamic variables independently associated with all-cause mortality. Candidate predictors were age, gender, New York Heart Association functional class (I to IV), heart rate, invasive PVR, invasive RA pressure, invasive mean pulmonary arterial pressure, and RV function echocardiographic parameters. The shared frailty

model was used with multivariate survival data where the unobserved frailty is shared among groups of individuals (random effects model for survival data). Receiver operating characteristic curves were used to determine diagnostic accuracy of standard RV function indices, RV strain parameters, and 3D-RVEF for the detection of RV failure hemodynamic signs (cardiac index  $<2$  L/min per  $m^2$ , RA pressure  $>15$ ) such as described in previous reports.<sup>23,24</sup> To assess the incremental value of 3DGFW-RVLS+3D-RVEF in predicting precapillary PH (pulmonary capillary wedge pressure  $<15$  mm Hg) over traditional echocardiographic parameters,  $\chi^2$  increase of the multivariate model in logistic regression analysis was determined. Global  $\chi^2$  value was measured in 3 steps. Step 1 included RVSP +MV-E/Ea (ratio of early diastolic mitral inflow velocity to early diastolic mitral annular velocity with values  $<12$  suggesting normal LV diastolic

function). Step 2 included RVSP+MV-E/Ea+3DGFW-RVLS. Step 3 included RVSP+MV-E/Ea+3DGFW-RVLS+3D-RVEF. Intra- and interobserver variability of strain and volumes measurements was evaluated in 10 randomly selected patients. To analyze intraobserver variability, measurements of parameters were made at multiple sites in different patients on 2 different occasions. For interobserver variability, a second investigator randomly made measurements at the above different sites without knowledge of other echocardiographic parameters. Variability was assessed using intraclass correlation coefficients for total agreement, with good agreement defined as  $>0.80$ . Mean values and SDs between the measurements were determined, and total agreement among the observation was obtained using intraclass correlation analysis.

## Results

Seventy-three patients with PH were included in the study. Ninety-four patients were initially evaluated. 2D and 3D speckle-tracking measurement from all segments and 3D RV volumetric analysis were not feasible in 8, 16, and 17 patients, respectively. Nine of the 17 patients excluded because 3D volume rendering was not allowed were patients with COPD. 3D feasibility was 82%, 2D strain feasibility was 92%, and 3D strain feasibility was 83%. Tricuspid regurgitation to estimate right-sided pressure was found in 73/94 patients (78%).

The baseline characteristics of PH patients and controls are given in Table 1. Echocardiographic parameters in PH patients and controls are presented in Table 2. TAPSE and FAC were lower and myocardial performance index was higher in PH patients. TV E/E' was increased and global and regional 3D-RVEF was reduced compared to controls. MV E/E' was significantly increased in MR patients compared to controls. Global and global-FW RVLS as well as right ventricular outflow tract longitudinal strain were significantly lower in all groups of patients than in controls. LVEF was unchanged, whereas LVED was larger in MR patients compared to controls. Reproducibility of 3D-STE analyses is summarized in Table 3.

The total duration of 3D-STE data analysis averaged  $8.3 \pm 1.7$  minutes, which was 33% less than the time used for 2D analyses ( $12.3 \pm 2.7$  minutes,  $P < 0.005$ ). Both image acquisition time ( $2.4 \pm 0.6$  minutes versus  $3.7 \pm 1.2$  minutes,  $P < 0.005$ ) and offline analysis time ( $5.9 \pm 1.6$  minutes versus  $8.6 \pm 1.9$  minutes,  $P < 0.001$ ) were significantly faster for 3D-STE compared with 2D-STE. Analysis time included calculation of areas and volumes and 2D-3D wall strains in different views from a single vendor-specific algorithm. Global LS measured by 2D-STE and 3D-STE showed a significant correlation

( $r = 0.79$ ,  $P < 0.005$ ). The correlation coefficient for segmental strain measured with 2D-STE and 3D-STE was 0.56 ( $P < 0.05$ ).

Both 3DGFW-RVLS and 3D-RVEF (Table 4) correlated similarly ( $P < 0.05$ ) with mean pulmonary artery pressure and PVR. A positive correlation was shown between 3DGFW-RVLS and RA pressure ( $P < 0.01$ ), and transpulmonary gradient ( $P = 0.03$ ). There was a negative correlation between 3DGFW-RVLS and pulmonary artery capacitance ( $P = 0.02$ ), and cardiac index ( $P < 0.01$ ). Tricuspid valve annular systolic velocity and RVFAC had a significant, but weaker, correlation with cardiac index ( $P < 0.05$ ) and no association with transpulmonary gradient or pulmonary vascular resistance. No correlation was obtained between RV outflow volume-strain parameters and right heart pressures.

Figure 3 analyzes RV global-free-wall longitudinal strain (GFW-RVLS), basal-free-wall longitudinal strain (BFW-RVLS), mid-free-wall longitudinal strain (MFW-RVLS), and apical-free-wall longitudinal strain (AFW-RVLS) in normal subjects and patients with PH (PAH, COPD, MR). Patients with precapillary PH (PAH, COPD) had lower global and regional peak systolic RV free-wall strain compared to patients with postcapillary PH (MR).

To assess the incremental value of 3DGFW-RVLS+3D-RVEF in predicting precapillary PH (pulmonary capillary wedge pressure  $< 15$  mm Hg) over traditional echocardiographic parameters, global  $\chi^2$  value was measured in 3 steps, as described in the Methods section. A significant improvement in global  $\chi^2$  value was noted (Figure 4) with strain and 3D parameters over traditional indices for the prediction of precapillary PH. The  $\chi^2$  values improved from 76.1 to 81.8 ( $P < 0.005$ ) and from 81.8 to 90.9 ( $P = 0.004$ ).

The diagnostic accuracy of RV strain and 3D-RVEF for detecting hemodynamic signs of RV failure (a composite of cardiac index  $< 2$  L/min per  $m^2$  and RA pressure  $> 15$ ) was shown by receiver-operating characteristic curves (Table 5). 3D-RVEF (0.89) had the highest area under the curve ( $P < 0.05$  compared to 3D-RVEF-inflow,  $P < 0.001$  compared to TAPSE), followed by 3D-GFW-RVAS (0.88), 3D-GFW-RVLS (0.88), GFW-RVLS (0.88), BFW-RVLS (0.85), AFW-RVLS (0.85), 3D-RVEF-apex (0.82), 3D-RVEF-inflow (0.81), 3D-RVEF-outflow (0.72), right ventricular outflow tract LS (0.69), and MFW RVLS (0.67).

Overall all-cause mortality at 2 years was 17.8% (13 patients). Proportional hazards modeling showed that death was associated with New York Heart Association functional class ( $P = 0.02$ ), age ( $P = 0.04$ ), male gender ( $P < 0.05$ ), invasive right atrial pressure ( $P < 0.001$ ), invasive pulmonary artery capacitance ( $P = 0.013$ ), invasive PVR ( $P = 0.02$ ), tricuspid valve annular systolic velocity ( $P = 0.03$ ), TAPSE ( $P = 0.03$ ), 3D-GFW-RVLS ( $P = 0.002$ ), and 3D-RVEF ( $P < 0.001$ ). In multivariate analysis, after adjusting for other predictors of mortality (significant predictors in univariate analysis), invasive RA

**Table 2.** Echocardiographic Parameters in PH Patients and Controls

	PAH (n=25)		COPD (n=23)	MR (n=25)	Controls (n=30)	P Value
	SS (n=12)	CHD (n=13)				
RV/LV	1.25±0.25	1.21±0.27	1.02±0.29	0.96±0.21	0.68±0.14	<0.01*
LVEDV, mL	122±17	118±19	112±15	161±27	119±16	<0.05 <sup>†</sup>
LVEF, %	58.6±7.7	59.9±7.4	60.3±6.8	62.4±7.3	61.3±6.2	ns
MV E/E <sub>a</sub>	8.7±2.6	8.9±2.5	9.3±2.8	17.7±6.8	5.4±3.6	<0.01 <sup>†</sup>
RVFAC, %	32±10	32±13	35±9	36±10	49±14	<0.05*
TAPSE, mm	14±5	15±6	16±6	17±4	23±5	<0.05*
RVMPI	0.55±0.11	0.58±0.12	0.41±0.12	0.39±0.10	0.24±0.06	<0.05*
TV S <sub>a</sub> , cm/s	7.2±3.3	7.1±3.1	8.7±2.7	9.6±3.2	12.9±2.4	<0.05*
TV E <sub>a</sub> , cm/s	8.1±3.4	8.5±3.1	8.6±2.9	9.2±3.1	15.6±3.5	<0.05*
TV E/E <sub>a</sub>	15.1±1.7	14.3±1.9	12.3±1.4	10.9±1.1	8.3±0.9	<0.05*
RVSP, mm Hg	79±12	74±10	49±13	45±14	22±3	<0.01*
PVR, WU	6.5±2.5	6.1±2.2	4.2±1.3	2.1±0.8	1.3±0.4	<0.05*
PAC, mL/mm Hg	0.7±0.2	0.9±0.2	1.5±0.9	1.8±0.7	3.2±1.9	<0.01*
TR, grade 0 to 3	1.8±0.5	1.9±0.4	1.2±0.3	1.7±0.6	0.3±0.2	<0.05*
PAT, ms	63.1±12.1	68.3±11.4	85.8±12.7	92.2±6.4	129.8±24.3	<0.05*
3D-RVEDV, mL	191±46	199±54	143±31	152±28	78±17	<0.005*
3D-RVESV, mL	123±27	116±29	94±23	102±22	34±9	<0.005*
3D-RVEF, %	35.5±7.6	36.4±8.2	38.1±7.6	40.7±8.1	53.6±7.2	<0.0001 <sup>‡</sup> , <0.001 <sup>§  </sup> , <0.05 <sup>†</sup>
3D-RVEF-inflow, %	33.1±7.4	32.8±7.9	34.6±7.3	39.7±6.7	54.1±7.6	<0.001 <sup>‡</sup> , <0.005 <sup>§  </sup> , <0.05 <sup>†</sup>
3D-RVEF-outflow, %	45.2±9.8	44.9±8.7	47.4±9.2	46.3±6.8	55.7±8.5	<0.05*
3D-RVEF-apex, %	26.3±4.4	27.8±4.6	30.1±5.2	29.6±3.9	42.4±8.1	<0.01 <sup>†§§</sup> , <0.05 <sup>  </sup>
RVOT LS, %	-7.6±4.8	-7.3±4.4	-8.1±2.6	-7.9±3.9	-9.1±5.1	<0.05*
Global RVLS, %	-19.1±4.6	-19.6±4.1	-20.3±4.9	-21.7±4.1	-24.1±3.6	<0.05*
Apical-FW RVLS, %	-10.9±4.3	-11.7±4.1	-14.9±4.8	-14.6±5.1	-21.7±4.6	<0.0001 <sup>‡</sup> , <0.0005 <sup>§</sup> , <0.01 <sup>†  </sup>
Mid-FW RVLS, %	-18.2±6.4	-18.9±6.7	-23.4±6.9	-22.5±7.6	-25.3±4.3	<0.05 <sup>‡</sup>
Basal-FW RVLS, %	-11.8±7.8	-12.8±7.4	-16.3±8.3	-20.9±7.8	-26.8±4.2	<0.0005 <sup>‡§</sup> , <0.001 <sup>  </sup> , <0.05 <sup>†</sup>
Global-FW RVLS, %	-17.7±4.9	-18.6±5.1	-19.2±4.7	-20.8±4.4	-25.9±5.7	<0.0001 <sup>‡§</sup> , <0.001 <sup>  </sup> , <0.01 <sup>†</sup>
3D Global RVLS, %	-17.1±4.3	-17.4±4.9	-18.9±4.8	-20.3±4.1	-22.4±3.5	<0.05*
3D Global-FW RVLS, %	-16.2±5.1	-17.1±5.2	-18.4±4.4	-19.7±3.9	-23.8±5.8	<0.0001 <sup>‡§</sup> , <0.001 <sup>  </sup> , <0.01 <sup>†</sup>
3D Global-FW AS, %	-22.4±5.3	-23.9±5.1	-24.7±4.8	-25.9±4.7	-34.6±5.8	<0.0001 <sup>‡§</sup> , <0.001 <sup>  </sup> , <0.01 <sup>†</sup>

3D indicates three-dimensional; AS, area strain; CHD, congenital heart disease; COPD, chronic obstructive pulmonary disease; E, inflow early diastolic velocity; E<sub>a</sub>, annular early diastolic velocity; FW, free wall; LV, left ventricular; LVEDV, left ventricular end-diastolic volume; LVEF, left ventricular ejection fraction; MR, mitral regurgitation; MV, mitral valve; PAC, pulmonary artery capacitance; PAH, pulmonary arterial hypertension; PAT, pulmonary acceleration time; PH, pulmonary hypertension; PVR, pulmonary vascular resistance; RV, right ventricular; RV/LV, ratio of RV to LV end-diastolic diameters (4-chamber view); RVEDV, right ventricular end-diastolic volume; RVEF, right ventricular ejection fraction; RVESV, right ventricular end-systolic volume; RVFAC, right ventricular fractional area change; RVLS, right ventricular longitudinal strain; RVMPI, right ventricular myocardial performance index; RVOT LS, right ventricular outflow tract longitudinal strain; RVSP, right ventricular systolic pressure; S<sub>a</sub>, annular systolic velocity; SS, systemic sclerosis; TAPSE, tricuspid annular plane systolic excursion; TR, tricuspid regurgitation; TV, tricuspid valve; WU, Wood units.

\*All vs controls.

<sup>†</sup>MR vs controls.

<sup>‡</sup>SS vs controls.

<sup>§</sup>CHD vs controls.

<sup>||</sup>COPD vs controls.

pressure (hazard ratio 6.2,  $P=0.001$ , 95% confidence interval 3.15 to 10.27), 3D-GFW-RVLS (hazard ratio 4.6,  $P=0.004$ , 95% CI 2.79 to 8.38), and 3D-RVEF (hazard ratio 5.3,  $P=0.002$ , 95% CI 2.85 to 9.89) were independent predictors of mortality.

## Discussion

The results of the present study are as follows: (1) In chronic PH setting, 3DE and STE parameters can detect global and

**Table 3.** Reproducibility of 3D and 2D-3D-STE Echocardiographic Analyses in a Subset of 10 Randomly Selected Patients With PH

Variable	Intraobserver			Interobserver		
	Mean Difference±SD	ICC	CV (%)	Mean Difference±SD	ICC	CV (%)
3D-RVEDV, mL	4.9±2.9	0.93	1.32	5.3±2.8	0.89	1.82
3D-RVESV, mL	5.7±3.6	0.87	1.95	5.9±3.9	0.82	2.41
3D-RVEF, %	5.9±3.8%	0.89	2.94	6.4±4.1	0.86	2.98
Global RVLS, %	6.0±2.9%	0.83	2.42	6.7±2.8%	0.77	3.81
Global-FW RVLS, %	5.4±3.1%	0.87	2.56	6.5±3.5%	0.83	2.95
Basal-FW RVLS, %	5.5±2.6%	0.85	2.92	5.5±2.7%	0.79	2.25
Mid-FW RVLS, %	6.1±2.6%	0.83	3.26	6.5±2.5%	0.78	3.47
Apical-FW RVLS, %	5.3±3.7%	0.86	2.34	5.9±3.5%	0.83	2.17
3D Global-FW RVLS, %	5.1±2.4%	0.92	1.87	6.0±3.1%	0.85	2.38
3D Global-FW AS, %	5.2±2.2%	0.91	2.12	5.9±2.5%	0.85	2.59

2D indicates two-dimensional; 3D, three-dimensional; AS, area strain; CV, coefficient of variation (calculated as the difference of repeated measurements expressed as a percentage of the mean); FW, free wall; ICC, intraclass correlation coefficient for absolute agreement; PH, pulmonary hypertension; RVEDV, right ventricular end-diastolic volume; RVEF, right ventricular ejection fraction; RVESV, right ventricular end-systolic volume; RVLS, right ventricular longitudinal strain; STE, speckle-tracking echocardiography.

**Table 4.** Correlation of RV Function Echocardiographic Parameters With Invasive Hemodynamic Variables

Right Heart Catheterization Data	RVFAC		TV-Sa		3D-GFW-RVLS		3D-RVEF	
	r Value	P Value	r Value	P Value	r Value	P Value	r Value	P Value
Mean PAP, mm Hg	−0.24	0.06	−0.31	<0.05	0.47	<0.05	−0.51	<0.05
PVR, WU	−0.19	0.08	−0.22	0.06	0.51	<0.05	−0.53	<0.05
TPG, mm Hg	−0.23	0.07	−0.24	0.06	0.50	0.03	−0.52	0.04
PAC, mL/mm Hg	0.22	0.07	0.29	<0.05	−0.54	0.02	0.55	0.02
Mean RAP, mm Hg	−0.32	<0.05	−0.36	<0.05	0.63	<0.01	−0.64	<0.01
CI, L/min per m <sup>2</sup>	0.38	<0.05	0.42	<0.05	−0.61	<0.01	0.60	<0.01

CI indicates cardiac index; 3D, three-dimensional; GFW-RVLS, global free-wall right ventricular longitudinal strain; PAC, pulmonary artery capacitance; PAP, pulmonary artery pressure; PVR, pulmonary vascular resistance; RAP, right atrial pressure; RVEF, right ventricular ejection fraction; RVFAC, right ventricular fractional area change; TPG, transpulmonary pressure gradient; TV-Sa, tricuspid valve annular systolic velocity; WU, Wood units.

regional RV dysfunction; (2) different forms of PH (precapillary, postcapillary) can differently affect RV deformation; and (3) 3DE and STE parameters are more powerful predictors of hemodynamic signs of RV failure compared to conventional RV indices.

## Previous Studies

Despite the prominent role of RV in PH prognosis, little is known about segmental patterns of RV function, and literature results have been conflicting. Previous studies using tissue Doppler imaging, STE, and 3DE<sup>6–9,21,25–29</sup> reported various patterns of RV remodeling in patients with chronic PH. A reduced apical RV longitudinal strain allowed feasible and reliable estimation of PH and appeared helpful to distinguish between pre- and postcapillary PH.<sup>26</sup> An apical dysfunction was also emphasized by magnetic resonance imaging (MRI)

studies.<sup>27</sup> Other authors showed moderate or severe RV dysfunction with decrease of strain of the basal segment of the RV free wall in patients with COPD<sup>6</sup> and PH of mixed etiologies.<sup>21,25</sup> There was improvement in regional 2D deformation parameters with long-term oral vasodilator therapy.<sup>21</sup> Low values of RV lateral free-wall 2D strain were found in patients with arterial and thromboembolic PH.<sup>8</sup> The importance of RV outflow tract function has been stressed by STE and MRI studies<sup>20,28</sup> showing increase of infundibular wall stress and decrease of fractional wall thickening in patients with PH of different etiologies. Serial quantitative assessment of RV function by strain<sup>29</sup> independently predicted clinical deterioration and mortality in patients with PAH after the institution of medical therapy.

The use of 3DE in the assessment of chronic PH<sup>4,30</sup> showed a different extent of contribution to the overall systolic function for the inflow, apical, and outflow tract

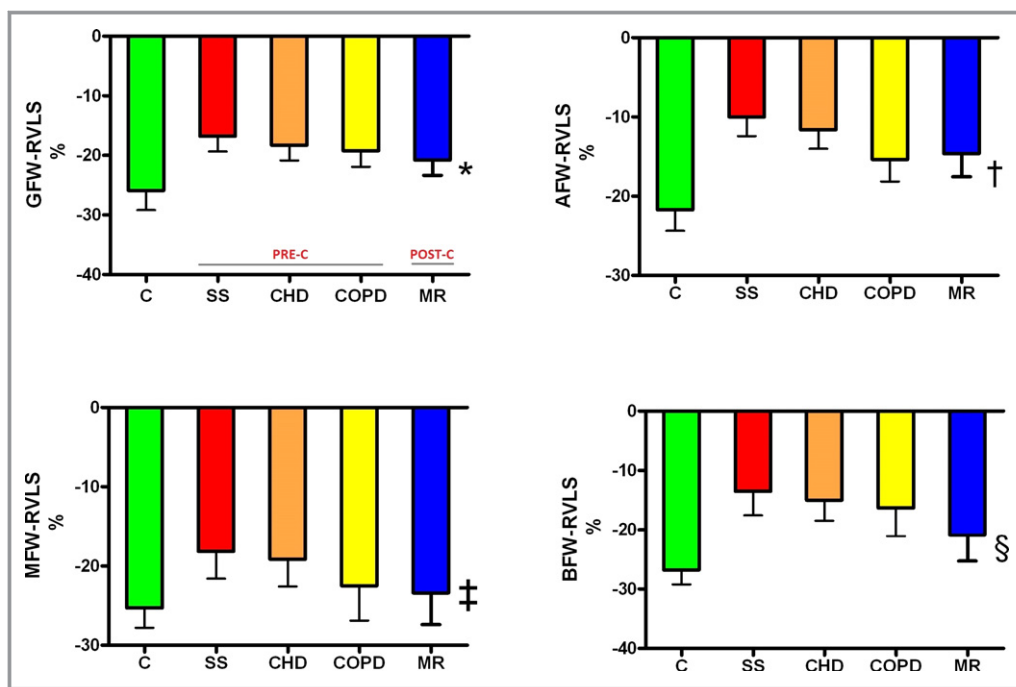


**Figure 3.** Bar graph depicting global and segmental strain changes in RV free wall in PH patients. RV global-free-wall longitudinal strain (GFWRVLS, top left) with higher decrease of RV global strain in precapillary PH (pre-c) compared to postcapillary PH (post-c). Apical-free-wall longitudinal strain (AFWRVLS, top right), mid-free-wall longitudinal strain (MFWRVLS, bottom left), and basal-free-wall longitudinal strain (BFWRVLS, bottom right) in normal subjects and patients with PH and RV segmental involvement. \*SS vs C:  $P < 0.0001$ ; CHD vs C:  $P < 0.0001$ ; COPD vs C:  $P < 0.001$ ; MR vs C:  $P < 0.01$ . †SS vs C:  $P < 0.0001$ ; CHD vs C:  $P < 0.0005$ ; COPD vs C:  $P < 0.01$ ; MR vs C:  $P < 0.01$ . ‡SS vs C:  $P < 0.001$ ; CHD vs C:  $P < 0.001$ ; COPD vs C: not significant; MR vs C: not significant. §SS vs C:  $P < 0.0005$ ; CHD vs C:  $P < 0.0005$ ; COPD vs C:  $P < 0.001$ ; MR vs C:  $P < 0.05$ . C indicates controls; CHD, congenital heart disease; COPD, chronic obstructive pulmonary disease; MR, mitral regurgitation; PH, pulmonary hypertension; RV, right ventricular; SS, systemic sclerosis.

compartments. Other studies described a significant association of 3D longitudinal strain<sup>10</sup> and area strain<sup>11</sup> with RVEF and a prognostic value independent of other variables.

## Present Study

Our report differs from previous literature in some respects. First, we analyzed comparatively the diagnostic accuracy of 3DE and 2D-3D-strain indices showing a better association with hemodynamic variables reflecting right heart failure than standard echo indices. To the best of our knowledge, this is the first study assessing the relation between these echocardiographic indices and the hemodynamic parameters indicative of RV failure. Second, RV strain impairment was more marked in patients with precapillary PH and less pronounced in patients with postcapillary PH and LV diastolic dysfunction and, even if overlap between groups limits its clinical utility, this finding showed an additional value compared to standard echo parameters, and this is of interest since current guidelines point out the importance of early diagnosis of precapillary PH and differentiation from other PH entities.<sup>1,2,26</sup>

Third, the apex involvement was a constant feature of RV dysfunction in chronic PH. This pattern is different from that seen in the acute pulmonary embolism setting as reported by ourselves<sup>31</sup> and others,<sup>32</sup> where reduced RV free wall contraction is found with preserved apical wall motion on 2DE. No bulging of the mid-RV free wall relative to the apex and base occurs in chronic PH since RV hypertrophy may limit shape changes and tethering effects.

The global and regional RV deformation patterns that we found in chronic PH can be explained by the complex and different pathophysiologic mechanisms in PH groups.<sup>33-38</sup> To group PH entities according to their pathophysiological-clinical mechanisms and response to medical therapy certainly helps clinical practice, although it is an oversimplification since differences exist within various subgroups. Systemic sclerosis-associated pulmonary artery hypertension (PAH-SS) has a poorer prognosis<sup>33</sup> than that of other types of PH,<sup>34</sup> with a median survival of 3 years. This could be explained by intrinsic myocardial involvement of the disease related to abnormal collagen deposition, or an increased vulnerability to ischemia due to coronary vasculopathy in

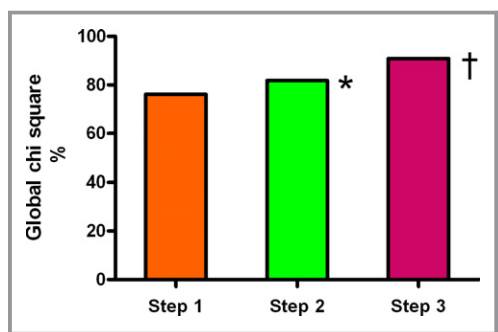


**Figure 4.** Incremental value of three-dimensional RV ejection fraction (3D-RVEF) and global-free-wall RV longitudinal strain (3DGFW-RVLS) over standard echocardiographic variables in predicting precapillary PH (PCWP <15 mm Hg). Step 1 included RVSP (right ventricular systolic pressure)+MV-E/E<sub>a</sub> (ratio of early diastolic mitral inflow velocity to early diastolic mitral annular velocity: values <12 suggest normal LV diastolic function). Step 2 included RVSP+MV-E/E<sub>a</sub>+3DGFW-RVLS. Step 3 included RVSP+MV-E/E<sub>a</sub>+3DGFW-RVLS+3D-RVEF. \*Step 1 vs step 2:  $\chi^2$  values 76.1 vs 81.8,  $P<0.005$ ; †Step 2 vs step 3:  $\chi^2$  values 81.8 vs 90.9,  $P=0.004$ . LV indicates left ventricular; MV, mitral valve; PCWP, pulmonary capillary wedge pressure; PH, pulmonary hypertension; RV, right ventricular.

addition to enhanced pulmonary vascular resistive and/or pulsatile loading. Patients with systemic sclerosis-associated pulmonary artery hypertension had higher values of pulmonary artery pressure and PVR, lower values of pulmonary artery capacitance, a more diffuse impairment in RV strain, and lower strain values compared to PAH-congenital heart disease, COPD, and MR patients. Actually, disorders associated with chronic lung disease or hypoxia are generally characterized by moderate PH, and RV dysfunction is characterized by hypertrophy with preserved cardiac function.<sup>35</sup> Nevertheless, RV failure can occur during disease exacerbations or when multiple comorbidities are present. PH is only mildly elevated also in chronic MR; it develops after the increased left atrial pressure (postcapillary), and the right ventricle is less dilated compared to PAH.<sup>36</sup> However, the presence of PH secondary to MR is a determinant of long-term survival, and RVEF has been shown to be an independent predictor of survival in patients with heart failure. The findings of our study are in line with previous reports<sup>4,28</sup> that described different global and regional RV changes in patients with different RV pressure overload.

In our population, both 2D-STE and 3D-STE were shown to be more sensitive to detect subtle myocardial damage compared to conventional indices of RV function. 3D area strain is a combination of longitudinal and circumferential function and has already been validated as a useful measurement of LV function.<sup>39</sup> Since it has integrated

2-directional components of myocardial deformation (longitudinal and circumferential), area strain might decrease the tracking error and emphasize synergistically the magnitude of deformation. Thus it is reasonable to expect that deteriorated ventricular function can be detected at an earlier stage by using 3D speckle-tracking analysis in comparison with 1-directional strain.<sup>40</sup> However, the superiority of 3D-STE over 2D-STE for the evaluation of all 3 components of LV deformation (longitudinal, circumferential, and radial) has been questioned.<sup>41</sup> The 3D mode avoids foreshortening of apical views, consumes less time in data acquisition, helps to solve the problem of out-of-plane motion present in the 2D modality tracking motion of speckles in all 3 dimensions, but this advantage is achieved at the expense of lower volume rate. Similar considerations can be made for the right ventricle; however, our results showed that the new 3D-STE measurements had strong associations with hemodynamic parameters indicative of RV failure, albeit we did not find any superior clinical advantage over 2D-STE except for a more rapid acquisition and offline-analysis time.

Our finding is partially coincident with previous research<sup>3,4,30,37</sup> suggesting that the change of volume and systolic function was at least in part related to high RV afterload caused by increased pulmonary artery pressure and PVR and existed in all of the 3 RV compartments. Furthermore, we showed that decrease in RV strain can be localized at the regional level (basal, apical) or widespread in the RV free wall. The decrease of EF and strain in the body and inflow compartment compared to controls were more significant than those in the outflow chamber. The early impairment of RV inflow systolic function could be explained by the predominant role of inflow contraction in RV global performance, and this is in keeping with the phylogenetic research that showed<sup>37</sup> that the RV sinus (inflow and body) compartments developed a million years after the outflow compartment, probably as an adaptation of the cardiovascular system to breathing air.

The moderate correlation we obtained between PVR and RVEF is in keeping with previous studies<sup>42</sup> that showed that in chronic PH, RV function does not fully adapt to changes in vascular properties and can decline independent of PVR, and RV contractility may increase during early PH and then decrease in a more advanced stage when pulmonary artery pressures fail to increase further. Other factors may play an important role in the changes in RVEF over time, including older age, genetic differences in RV adaptation to pressure overload, and ventricular wall tension.<sup>42</sup> Moreover, correlations between RV function echocardiographic parameters and mean pulmonary artery pressure obtained via catheterization may be stronger in pulmonary hypertensive patients solely with right-sided disease and weaker in mixed populations including patients with LV overload and/or dysfunction.<sup>7</sup>

**Table 5.** Results of Receiver-Operating Characteristic Curves Comparing Different Echocardiographic Parameters in all PH Cohorts for Their Accuracy to Predict Hemodynamic Parameters of RV Failure

Parameter	AUC	95% CI	P Value	Cutoff	Sensitivity	Specificity
2D-TVI						
RVFAC	0.62	0.47 to 0.86	0.08	38%	72	60
TV-Sa	0.66	0.52 to 0.89	0.06	9.2 cm/s	75	65
TAPSE	0.67	0.53 to 0.88	0.05	16 mm	76	64
Strain						
RVOT LS	0.69	0.51 to 0.82	0.04	−7.4%	79	64
Mid-FW RVLS	0.67	0.63 to 0.90	0.06	−18%	76	65
Apical-FW RVLS	0.85	0.69 to 0.97	0.03	−16%	86	76
Basal-FW RVLS	0.85	0.72 to 0.96	0.02	−19%	86	78
Global-FW RVLS	0.88	0.69 to 0.98	0.01	−18%	89	74
3D Global-FW RVLS	0.88*	0.71 to 0.97	0.01	−17%	89	77
3D Global-FW AS	0.88*	0.72 to 0.99	0.01	−27%	89	78
3D volumes						
3D-RVEF-outflow	0.72	0.58 to 0.87	0.05	42%	77	64
3D-RVEF-apex	0.81	0.61 to 0.91	0.04	28%	81	73
3D-RVEF-inflow	0.82	0.76 to 0.98	0.03	36%	82	75
3D-RVEF	0.89 <sup>†</sup>	0.68 to 0.99	<0.01	39%	90	83

2D indicates two-dimensional; 3D, three-dimensional; AS, area strain; AUC, area under the curve; FW RVLS, free-wall right ventricular longitudinal strain; PH, pulmonary hypertension; RVEF, right ventricular ejection fraction; RVFAC, right ventricular fractional area change; RVOT LS, right ventricular outflow tract longitudinal strain; TAPSE, tricuspid annular plane systolic excursion; TVI, tissue velocity imaging; TV-Sa, tricuspid valve annular systolic velocity.

\* $P < 0.05$  compared to Basal-FW RVLS,  $P < 0.005$  compared to TAPSE.

<sup>†</sup> $P < 0.05$  compared to 3D-RVEF-inflow,  $P < 0.001$  compared to TAPSE.

We have already reported<sup>18,31</sup> that the newer technologies appear to be superior to conventional technologies, including RVFAC, TAPSE, and myocardial performance index. In our cohort of patients with chronic PH, the assessment of 3D RVEF and strain gave us valuable information on global and regional RV function with better diagnostic accuracy in predicting RV failure hemodynamics compared to the other methods. Also, in our study we have found some common strong prognostic factors with chronic PH, such as age, New York Heart Association functional class, invasive right atrial pressure, pulmonary artery capacitance, pulmonary vascular resistance, TAPSE, 3D-GFW-RVLS, and 3D-RVEF. The results concerning the prognostic value of pulmonary artery capacitance provide further evidence that pulsatile components (pulmonary artery capacitance) of RV afterload give additional information compared to the static part (PVR) of RV afterload.<sup>14,43</sup> STE and 3D echocardiographic parameters tended to be associated with adverse events in univariate analysis and were independently associated with adverse events in multivariate analysis, and these data are in keeping with recent reports<sup>11</sup> showing that reduced RV strain was associated with poor outcome in PH patients.

## Clinical Implications

We have shown that in chronic PH patients, 3D RV volumes and 2D-3D strains are better predictors of the hemodynamic indices of RV failure compared to conventional RV parameters as well as better predictors of mortality. Both RV global function parameters and regional strain indices of the inflow region and apex appeared to detect early signs of ventricular failure. Their use could improve the evaluation of subtle RV changes when TAPSE, tricuspid valve annular systolic velocity, and FAC are not conclusive or in the first stages of PH when TAPSE is known to be still normal. The described cutoff values for global and regional RV echo parameters (3D-RVEF 39%, 3D global-FW RVLS −17%, basal-FW RVLS −19%, apical-FW RVLS −16%) may allow PH patients to be followed serially and to assess the response to medical therapy.

## Limitations

Our study did have some limitations. First, RV 2D-strain analysis software was used assuming that the LV algorithm could be transferred to the right ventricle. However, it has been applied to the RV in several clinical studies,<sup>8,16,17</sup> albeit

reproducibility should undergo further validation. Second, STE is dependent both on frame rate and image resolution. We used frame rates in the range of 60 to 100 Hz, which is a lower value than a frame rate suitable for Doppler strain. However, STE may overcome some tissue Doppler limitations because it is less affected by passive translational motion or tethering in the assessment of myocardial thickening. Third, although the problem of variations between the different systems and vendors was recently stressed in terms of speckle-tracking analysis,<sup>44</sup> a comparison of data obtained using the various systems would be appropriate, and this problem will require collaboration between manufacturers. Fourth, 3D-STE software has been designed for LV assessment, and development of a specific RV software would be desirable. Fifth, cardiac catheterization and echocardiographic measurements were not obtained simultaneously, and potentially measurements in different hemodynamic states might have occurred. However, the mean time between echo and catheterization was 1.4 days; thus, it is very unlikely that conclusions were affected by this delay. An additional limitation was that cardiac output was measured invasively using thermodilution, and this method may lack accuracy in patients with PH due to congenital intracardiac shunts or in patients with significant tricuspid regurgitation. However, tricuspid regurgitation was mild in the majority of our patients, and also it has been shown that this method is equally as accurate as other methods of measuring cardiac output even in the presence of tricuspid regurgitation.<sup>22</sup> Another limitation was that the accuracy of 3D volume and EF is less reliable in significantly dilated and dysfunctional ventricles because limited data are available in the literature.<sup>3,4</sup> The 3D RV endocardial border identification may be challenging as echo dropouts frequently occur, especially of the anterior wall and outflow tract, and is even more challenging in patients with dilated right ventricles, because the endocardial border may be blurred due to the increased distance from the transducer to the RV wall. The last limitation was the lack of comparison with cardiac MRI. Previous studies showed a good correlation between 3DE and MRI volumes in patients with PH<sup>3</sup> but future studies correlating RV 3D-MRI tagging with 3D-STE would be desirable.

## Conclusions

In PH patients, the quantitative assessment of global and regional RV function by 3D and STE provided us useful hemodynamic and prognostic informations. The future software improvements, the improving tracking ability of the STE and 3D systems, and availability of a greater number of patients with a longer follow-up will refine the evaluation of RV dysfunction in chronic PH.

## Disclosures

None.

## References

- Galiè N, Hoeper MM, Humbert M, Torbicki A, Vachiery JL, Barbera JA, Beghetti M, Corris P, Gaine S, Gibbs JS, Gomez-Sanchez MA, Jondeau G, Klepetko W, Opitz C, Peacock A, Rubin L, Zellweger M, Simonneau G; ESC Committee for Practice Guidelines (CPG). Guidelines for the diagnosis and treatment of pulmonary hypertension: the Task Force for the Diagnosis and Treatment of Pulmonary Hypertension of the European Society of Cardiology (ESC) and the European Respiratory Society (ERS), endorsed by the International Society of Heart and Lung Transplantation (ISHLT). *Eur Heart J*. 2009;30:2493–2537.
- McLaughlin VV, Archer SL, Badesch DB, Barst RJ, Farber HW, Lindner JR, Mathier MA, McGoon MD, Park MH, Rosenson RS, Rubin LJ, Tapson VF, Varga J, Harrington RA, Anderson JL, Bates ER, Bridges CR, Eisenberg MJ, Ferrari VA, Grines CL, Hlatky MA, Jacobs AK, Kaul S, Lichtenberg RC, Lindner JR, Moliterno DJ, Mukherjee D, Pohost GM, Rosenson RS, Schofield RS, Shubrooks SJ, Stein JH, Tracy CM, Weitz HH, Wesley DJ. ACCF/AHA 2009 expert consensus document on PH. A Report of the American College of Cardiology Foundation Task Force on Expert Consensus Documents and the American Heart Association. *Circulation*. 2009;119:2250–2294.
- Grapsa J, O'Regan DP, Pavlopoulos H, Durighel G, Dawson D, Nihoyannopoulos P. Right ventricular remodelling in pulmonary arterial hypertension with three-dimensional echocardiography: comparison with cardiac magnetic resonance imaging. *Eur J Echocardiogr*. 2010;11:64–73.
- Grapsa J, Gibbs JS, Dawson D, Watson G, Patni R, Athanasiou T, Punjabi PP, Howard LS, Nihoyannopoulos P. Morphologic and functional remodeling of the right ventricle in pulmonary hypertension by real time three dimensional echocardiography. *Am J Cardiol*. 2012;109:906–913.
- Grapsa J, Gibbs JS, Cabrita IZ, Watson GF, Pavlopoulos H, Dawson D, Gin-Sing W, Howard LS, Nihoyannopoulos P. The association of clinical outcome with right atrial and ventricular remodelling in patients with pulmonary arterial hypertension: study with real-time three-dimensional echocardiography. *Eur Heart J Cardiovasc Imaging*. 2012;13:666–672.
- Vitarelli A, Conde Y, Cimino E, Stellato S, D'Orazio S, D'Angeli I, Nguyen BL, Padella V, Caranci F, Petrosianni A, D'Antoni L, Terzano C. Assessment of right ventricular function by strain rate imaging in chronic obstructive pulmonary disease. *Eur Respir J*. 2006;27:268–275.
- Rajagopalan N, Simon MA, Shah H, Mathier MA, López-Candales A. Utility of right ventricular tissue Doppler imaging: correlation with right heart catheterization. *Echocardiography*. 2008;25:706–711.
- Fukuda Y, Tanaka H, Sugiyama D, Ryo K, Onishi T, Fukuya H, Nogami M, Ohno Y, Emoto N, Kawai H, Hirata K. Utility of right ventricular free wall speckle-tracking strain for evaluation of right ventricular performance in patients with pulmonary hypertension. *J Am Soc Echocardiogr*. 2011;24:1101–1108.
- Rajagopal S, Forsha DE, Risum N, Hornik CP, Poms AD, Fortin TA, Tapson VF, Velazquez EJ, Kisslo J, Samad Z. Comprehensive assessment of right ventricular function in patients with pulmonary hypertension with global longitudinal peak systolic strain derived from multiple right ventricular views. *J Am Soc Echocardiogr*. 2014;27:657–665.
- Ozawa K, Funabashi N, Takaoka H, Tanabe N, Yanagawa N, Tatsumi K, Kobayashi Y. Utility of three-dimensional global longitudinal strain of the right ventricle using transthoracic echocardiography for right ventricular systolic function in pulmonary hypertension. *Int J Cardiol*. 2014;174:426–430.
- Smith BC, Dobson G, Dawson D, Charalampopoulos A, Grapsa J, Nihoyannopoulos P. Three-dimensional speckle tracking of the right ventricle: toward optimal quantification of right ventricular dysfunction in pulmonary hypertension. *J Am Coll Cardiol*. 2014;64:41–51.
- Lang RM, Bierig M, Devereux RB, Flachskampf FA, Foster E, Pellikka PA, Picard MH, Roman MJ, Seward J, Shanewise J, Solomon S, Spencer KT, St John Sutton M, Stewart W. Recommendations for chamber quantification: a report from the American Society of Echocardiography's Guidelines and Standards Committee and the Chamber Quantification Writing Group, developed in conjunction with the European Association of Echocardiography, a branch of the European Society of Cardiology. *J Am Soc Echocardiogr*. 2005;18:1440–1463.
- Abbas AE, Fortuin FD, Schiller NB, Appleton CP, Moreno CA, Lester SJ. A simple method for noninvasive estimation of pulmonary vascular resistance. *J Am Coll Cardiol*. 2003;4:1021–1027.
- Mahapatra S, Nishimura RA, Oh JK, McGoon MD. The prognostic value of pulmonary vascular capacitance determined by Doppler echocardiography in patients with pulmonary arterial hypertension. *J Am Soc Echocardiogr*. 2006;19:1045–1050.

15. Rudski LG, Lai WW, Afilalo J, Hua L, Handschumacher MD, Chandrasekaran K, Solomon SD, Louie EK, Schiller NB. Guidelines for the echocardiographic assessment of the right heart in adults: a report from the American Society of Echocardiography endorsed by the European Association of Echocardiography, a registered branch of the European Society of Cardiology, and the Canadian Society of Echocardiography. *J Am Soc Echocardiogr.* 2010;23:685–713.
16. Pirat B, McCulloch ML, Zoghbi WA. Evaluation of global and regional right ventricular systolic function in patients with pulmonary hypertension using a novel speckle tracking method. *Am J Cardiol.* 2006;98:699–704.
17. Teske AJ, Prakken NH, De Boeck BW, Velthuis BK, Martens EP, Doevendans PA, Cramer MJ. Echocardiographic tissue deformation imaging of right ventricular systolic function in endurance athletes. *Eur Heart J.* 2009;30:969–977.
18. Vitarelli A, Sardella G, Di Roma A, Capotosto L, De Curtis G, D’Orazio S, Cicconetti P, Battaglia D, Caranci F, De Maio M, Bruno P, Vitarelli M, De Chiara S. Assessment of right ventricular function by three-dimensional echocardiography and myocardial strain imaging in adult atrial septal defect before and after percutaneous closure. *Int J Cardiovasc Imaging.* 2012;28:1905–1916.
19. Vitarelli A, Capotosto L, Placanica G, Caranci F, Pergolini M, Zardo F, Martino F, De Chiara S, Vitarelli M. Comprehensive assessment of biventricular function and aortic stiffness in athletes with different forms of training by three-dimensional echocardiography and strain imaging. *Eur Heart J Cardiovasc Imaging.* 2013;14:1010–1020.
20. Calcutteea A, Lindqvist P, Soderberg S, Henein MY. Global and regional right ventricular dysfunction in pulmonary hypertension. *Echocardiography.* 2014;31:164–171.
21. Borges AC, Knebel F, Eddicks S, Panda A, Schattke S, Witt C, Baumann G. Right ventricular function assessed by two-dimensional strain and tissue Doppler echocardiography in patients with pulmonary arterial hypertension and effect of vasodilator therapy. *Am J Cardiol.* 2006;98:530–534.
22. Hoepfer MM, Maier R, Tongers J, Niedermeyer J, Hohlfeld JM, Hamm M, Fabel H. Determination of cardiac output by the Fick method, thermodilution, and acetylene rebreathing in pulmonary hypertension. *Am J Respir Crit Care Med.* 1999;160:535–541.
23. Orens JB, Estenne M, Arcasoy S, Conte JV, Corris P, Egan JJ, Egan T, Keshavjee S, Knoop C, Kotloff R, Martinez FJ, Nathan S, Palmer S, Patterson A, Singer L, Snell G, Studer S, Vachiery JL, Glanville AR; Pulmonary Scientific Council of the International Society for Heart and Lung Transplantation. International guidelines for the selection of lung transplant candidates: 2006 update—a consensus report from the Pulmonary Scientific Council of the International Society for Heart and Lung Transplantation. *J Heart Lung Transplant.* 2006;25:745–755.
24. Lahm T, McCaslin CA, Wozniak TC, Ghumman W, Fadl YY, Obeidat OS, Schwab K, Meldrum DR. Medical and surgical treatment of acute right ventricular failure. *J Am Coll Cardiol.* 2010;56:1435–1446.
25. Brili S, Stamatopoulos I, Misailidou M, Chrysohoou C, Tousoulis D, Tatsis I, Stefanadis C. Longitudinal strain curves in the RV free wall differ in morphology in patients with pulmonary hypertension compared to controls. *Int J Cardiol.* 2013;167:2753–2756.
26. Hammerstingl C, Schueler R, Bors L, Momcilovic D, Pabst S, Nickenig G, Skowasch D. Diagnostic value of echocardiography in the diagnosis of pulmonary hypertension. *PLoS One.* 2012;7:e38519.
27. Fernandez-Friera L, Garcia-Alvarez A, Guzman G, Bagheriannejad-Esfahani F, Malick W, Nair A, Fuster V, Garcia MJ, Sanz J. Apical right ventricular dysfunction in patients with pulmonary hypertension demonstrated with magnetic resonance. *Heart.* 2011;97:1250–1256.
28. Simon MA, Deible C, Mathier MA, Lacomis J, Goitein O, Shroff SG, Pinsky MR. Phenotyping the right ventricle in patients with pulmonary hypertension. *Clin Transl Sci.* 2009;2:294–299.
29. Hardegree EL, Sachdev A, Villarraga HR, Frantz RP, McGoon MD, Kushwaha SS, Hsiao JF, McCully RB, Oh JK, Pellikka PA, Kane GC. Role of serial quantitative assessment of right ventricular function by strain in pulmonary arterial hypertension. *Am J Cardiol.* 2013;111:143–148.
30. Calcutteea A, Chung R, Lindqvist P, Hodson M, Henein MY. Differential right ventricular regional function and the effect of pulmonary hypertension: three-dimensional echo study. *Heart.* 2011;97:1004–1011.
31. Vitarelli A, Barilla F, Capotosto L, D’Angeli I, Truscelli G, De Maio M, Ashurov R. Right ventricular function in acute pulmonary embolism: a combined assessment by three-dimensional and speckle tracking echocardiography. *J Am Soc Echocardiogr.* 2014;27:329–338.
32. Ichikawa K, Dohi K, Sugiura E, Sugimoto T, Takamura T, Ogihara Y, Nakajima H, Onishi K, Yamada N, Nakamura M, Nobori T, Ito M. Ventricular function and dyssynchrony quantified by speckle-tracking echocardiography in patients with acute and chronic right ventricular pressure overload. *J Am Soc Echocardiogr.* 2013;26:483–492.
33. Tedford RJ, Mudd JO, Girdis RE, Mathai SC, Zaiman AL, Hosten-Harris T, Boyce D, Kelemen BW, Bacher AC, Shah AA, Hummers LK, Wigley FM, Russell SD, Saggat R, Saggat R, Maughan WL, Hassoun PM, Kass DA. Right ventricular dysfunction in systemic sclerosis associated pulmonary arterial hypertension. *Circ Heart Fail.* 2013;6:953–963.
34. Barst RJ, Ivy DD, Foreman AJ, McGoon MD, Rosenzweig EB. Four- and seven-year outcomes of patients with congenital heart disease-associated pulmonary arterial hypertension (from the REVEAL Registry). *Am J Cardiol.* 2014;113:147–155.
35. Tanaka Y, Hino M, Mizuno K, Gemma A. Evaluation of right ventricular function in patients with COPD. *Respir Care.* 2013;58:816–823.
36. Le Tourneau T, Deswarte G, Lamblin N, Foucher-Hosseine C, Fayad G, Richardson M, Polge AS, Vannesson C, Topilsky Y, Juthier F, Trochu JN, Enriquez-Sarano M, Bauters C. Right ventricular systolic function in organic mitral regurgitation: impact of biventricular impairment. *Circulation.* 2013;127:1597–1608.
37. Kong D, Shu X, Dong L, Pan C, Cheng L, Yao H, Zhou D. Right ventricular regional systolic function and dyssynchrony in patients with pulmonary hypertension evaluated by three-dimensional echocardiography. *J Am Soc Echocardiogr.* 2013;26:649–656.
38. Hilde JM, Skjorten I, Grøtta OJ, Hansteen V, Melsom MN, Hisdal J, Humerfelt S, Steine K. Right ventricular dysfunction and remodeling in chronic obstructive pulmonary disease without pulmonary hypertension. *J Am Coll Cardiol.* 2013;62:1103–1111.
39. Kleijn SA, Aly MFA, Terwee CB, van Rossum AC, Kamp O. Three-dimensional speckle tracking echocardiography for automatic assessment of global and regional left ventricular function based on area strain. *J Am Soc Echocardiogr.* 2011;24:314–321.
40. Vitarelli A, Martino F, Capotosto L, Martino E, Colantoni C, Ashurov R, Ricci S, Conde Y, Maramao F, Vitarelli M, De Chiara S, Zanoni C. Early myocardial deformation changes in hypercholesterolemic and obese children and adolescents: a 2D and 3D speckle tracking echo study. *Medicine.* 2014;93:e71(1–10).
41. Altman M, Bergerot C, Aussoleil A, Davidsen ES, Sibellas F, Ovize M, Bonnefoy-Cudraz E, Thibault H, Derumeaux G. Assessment of left ventricular systolic function by deformation imaging derived from speckle tracking: a comparison between 2D and 3D echo modalities. *Eur Heart J Cardiovasc Imaging.* 2014;15:316–323.
42. van de Veerdonk MC, Kind T, Marcus JT, Mauritz GJ, Heymans MW, Bogaard HJ, Boonstra A, Marques KM, Westerhof N, Vonk-Noordegraaf A. Progressive right ventricular dysfunction in patients with pulmonary arterial hypertension responding to therapy. *J Am Coll Cardiol.* 2011;58:2511–2519.
43. Dupont M, Mullens W, Skouri HN, Abrahams Z, Wu Y, Taylor DO, Starling RC, Tang WH. Prognostic role of pulmonary arterial capacitance in advanced heart failure. *Circ Heart Fail.* 2012;5:778–785.
44. Manovel A, Dawson D, Smith B, Nihoyannopoulos P. Assessment of left ventricular function by different speckle-tracking software. *Eur J Echocardiogr.* 2010;11:417–421.